Joint Pathology Center
Veterinary Pathology Services

WEDNESDAY SLIDE CONFERENCE 2024-2025

Conference #19 29 January 2025

CASE I:

Signalment:
22 year old, female, Green anaconda (*Eunectes murinus*)

History:
This snake was humanely euthanized due to a persistent Ophidiomyces infection with clinical signs (not specified), despite over 6 months of treatment with terbinafine.

Gross Pathology:
Necropsy was performed by the clinicians, and formalin-fixed tissues were sent to our laboratory for histopathologic exam. The clinicians reported multifocal areas of brown discoloration on the ventral scales. Corneas were reported to be cloudy. There were multifocal yellow nodules in the lungs**.**

Laboratory Results:
Antemortem skin swab submitted to the Illinois Veterinary Diagnostic Laboratory was positive via qPCR for Ophidiomyces

Postmortem, panfungal PCR at the University of Florida did not detect Ophidiomyces in paraffin-embedded lung tissue.

Microscopic Description:
Randomly distributed in the lungs are multifocal to coalescing nodules composed of central areas of amorphous, eosinophilic to occasionally mineralized, necrotic debris. This central necrotic material is surrounded by moderate to high numbers of macrophages, with lymphocytes and plasma cells present at the periphery. In some granulomas, fungal hyphae that are 2-3 um wide, with parallel walls, septa, and occasional acute angle branching, stain positive with Grocott methenamine silver (GMS) and periodic-acid-Schiff (PAS) stains.

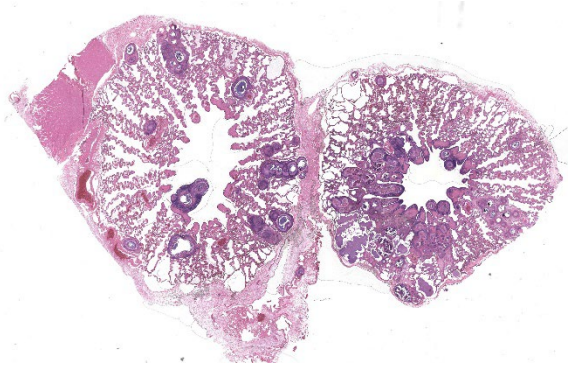

Figure 1-1. Lung, green anaconda. Scattered throughout the lung, there are numerous granulomas expanding the faveolar septa. (HE, 10X)

Contributor's Morphologic Diagnosis:
Lungs: Multifocal granulomatous pneumonia with fungi

Contributor's Comment:
This case highlights a granulomatous pneumonia caused by a fungus with histologic features consistent with *Ophidiomyces ophiodiicola*. The fungal infection is presumed to have originated from the dermal *Ophidiomyces ophiodiicola* infection detected antemortem via qPCR in dermal lesions found on this captive, green anaconda.

Figure 1-2. Lung, green anaconda. Coalescing granulomas expand the alveolar septa (HE, 111X)

Ophidiomyces ophiodiicola is the causative agent of "snake fungal disease". First described in eastern massasauga rattlesnakes in Illinois, USA, in 2011, it was originally characterized as an emerging infectious disease.[1,2] It has since been described in the eastern to mid-western United States, Canada, Europe, and in Australia.[2,3,4,5] However, recent reviews suggest that *O. ophiodiicola* may be a common, endemic disease that was previously uncharacterized, rather than an emerging infectious agent.[2,6] Retrospective testing found the earliest confirmed infection to be 1986, and there does not appear to be an increase over the last decade in the prevalence of *O. ophiodiicola* or change in its distribution, at least in North America.[2]

Originally classified within the chrysosporium anamorph of Nannizziopsis vriesii complex, it was initially unclear if *O. ophiodiicola* was a primary or opportunistic pathogen.[7] Later experimental infections of corn snakes with *O. ophiodiicola* confirmed a casual link between *O. ophiodiicola* and lesions consistent with those seen in wild snakes with snake fungal disease. In addition, they found that variation of described clinical signs in the literature may be explained by the stage of infection.[7] Increased frequency of molting, anorexia, and abnormal behaviors such as resting in conspicuous areas were also observed.[7]

The clinical presentation can vary, but typically, *O. ophiodiicola* produces a fungal dermatitis characterized by early superficial dermatitis and scale loss, and severe and chronic infections can result in extensive ulceration, facial swelling and disfiguration.[1,3,8] Histologically, lesions range from heterophilic to necrotizing epidermitis, with or without granulomatous dermatitis, granulomatous pneumonia, granulomatous endophthalmitis, and subcutaneous/intramuscular granulomas.[6] Systemic infections have been described.[9]

In addition to histopathology and histochemical stains, fungal culture and PCR are recommended for definitive diagnosis.[3] In this case antemortem dermal swabs were positive for *Ophidiomyces ophiodiicola* via qPCR. Postmortem panfungal PCR of paraffin-embedded lung tissue did not detect *Ophidiomyces ophiodiicola,* but did detect *Malassezia sp*, a presumed contaminant, given histologic features of the fungus. Given the antemortem qPCR positive, and histologic features, a presumptive diagnosis of granulomatous pneumonia due to *Ophidiomyces ophiodiicola* was made. It is likely that prolonged formalin fixation interfered with amplification of *Ophidiomyces ophiodiicola* in this case.

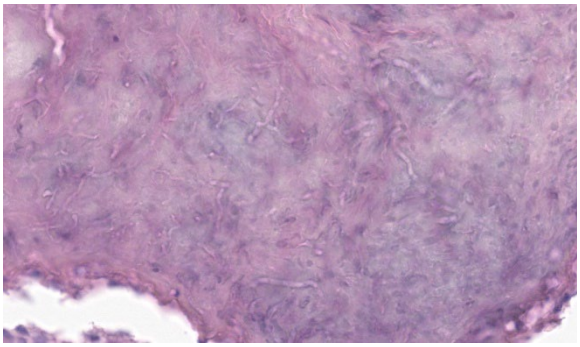

Figure 1-3. Lung, green anaconda. The outline of septate fungal hyphae may be seen within the central coagulum in several of the granulomas. (HE, 1336X)

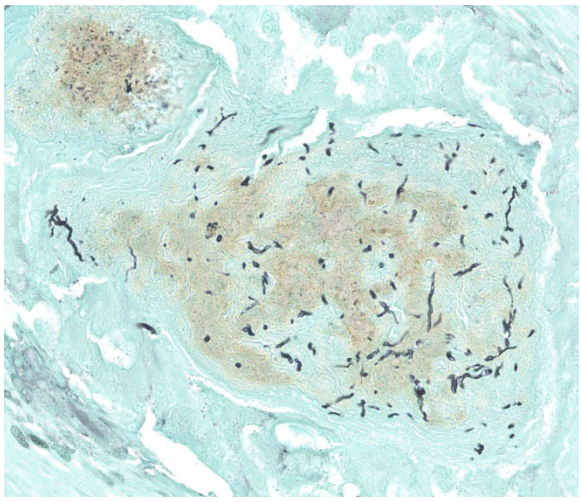

Figure 1-4. Lung, green anaconda. A GMS stain highlights the morphology of the fungal hyphae. (GMS, 637X)

Contributing Institution:
https://nmdeptag.nmsu.edu/labs/veterinary-diagnostic-services.html

JPC Diagnosis:
Lung: Pneumonia, granulomatous, chronic, multifocal, moderate, with fungal hyphae.

JPC Comment:
This week's moderator was Dr. Lauren Peiffer of Smithsonian's National Zoo and Conservation Biology Institute who explored bird and reptile cases with conference participants. This first case in a green anaconda is a rare look at a snake lung with marked ancillary changes to accompany prominent granulomas. The faveolar septa are expanded either by fibrosis and/or smooth muscle hyperplasia and contain hemosiderin-laden macrophages which reinforce the chronicity of the overall process. Fungal elements are apparent in select granulomas on H&E, but their mophology is better appreciated with GMS and PAS stains. In particular, PAS(with malachite green counterstain) was helpful for detailing septation and contour of hyphae which was consistent with *Ophidiomyces ophiodiicola*.

Dr. Peiffer discussed differentials for lung granulomas in snakes with mycobacteriosis being an important rule out. We performed modified Gram stains (Brown-Brenn, Brown-Hopps) and acid-fast stains (Fite-Faraco, Ziehl-Neelsen) which identified gram-positive bacilli with some granulomas that were highlighted with Fite-Faraco, but not Ziehl-Neelsen. These findings are consistent with *Mycobacterium* sp. and concurrent infectious agents are a common finding in granulomatous inflammation. Multiple species of mycobacteria have been reported in snakes, including *M. marinum*, *M. haemophilum*, *M. kansasii*, *M. chelonae*, and *M. leprae*.[10]

We agree with the contributor that the finding of *Malassezia* on the panfungal PCR is probably spurious and second the notion to compare the results of ancillary diagnostics in assessing their validity. *Malassezia restricta* is a common contaminant and in this case may have been preserved within the paraffin block or sampled from the operator or lab environment itself. The lack of recovery of *Ophidiomyces ophiodiicola* may reflect degradation of DNA in formalin – given the large number of hyphae present in section, we do not believe that prolonged antifungal therapy was probably not a factor.

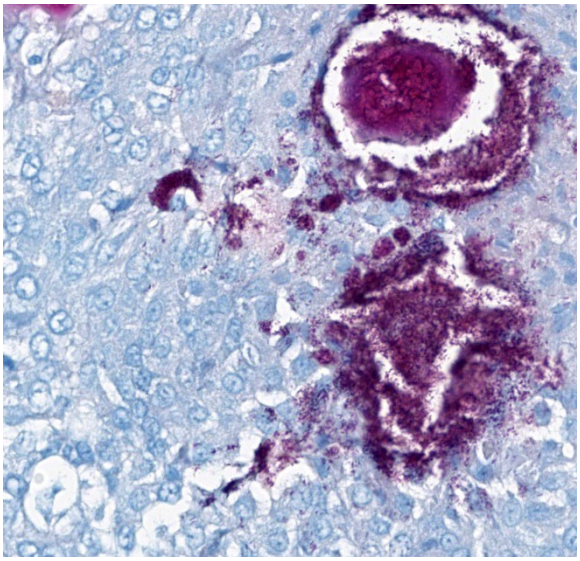

Figure 1-5. Lung, green anaconda. Some granulomas contain acid-fast bacilli. (Fite-Faraco, 858X)

References:

1. Allender MC, Dreslik M, Wylie S, Phillips C, Wylie DB, Maddox C, Delaney MA, Kinsel MJ. Chrysosporium sp. infection in eastern massasauga rattlesnakes. *Emerg Infect Dis*. 2011 Dec;17(12):2383-4.
2. Davy CM, Shirose L, Campbell D, Dillon R, McKenzie C, Nemeth N, et al. Revisiting Ophidiomycosis (Snake Fungal Disease) After a Decade of Targeted Research. *Front Vet Sci.* 2021; 8: 665805.
3. Ossiboff R. In: Pathology of Wildlife and Zoo Animals. Terio K, McAloose D, St. Leger J, eds. London, Academic Press, 2018: 912-914.
4. Franklinos LHV, Lorch JM, Bohuski E, Rodriguez-Ramos Fernandez J, Wright ON, Fitzpatrick L, Petrovan S, Durrant C, Linton C, Baláž et al. Emerging fungal pathogen Ophidiomyces ophiodiicola in wild European snakes. *Sci Rep.* 2017 Jun 19;7(1):3844
5. Sigler L, Hambleton S, Paré JA. Molecular characterization of reptile pathogens currently known as members of the chrysosporium anamorph of Nannizziopsis vriesii complex and relationship with some human-associated isolates. *J Clin Microbiol*. 2013 Oct;51(10):3338-57.
6. Anderson KB, Steeil JC, Neiffer DL, et al. Retrospective review of Ophidiomycosis (Ophidiomyces ophidiicola) at the Smithsonian's National Zoological Park (1983-2017). *Journal of Zoo and Wildlife Medicine.* 52(3), 997-1002
7. Lorch JM, Lankton J, Werner K, Falendysz EA, McCurley K, Blehert DS. Experimental Infection of Snakes with Ophidiomyces ophiodiicola Causes Pathological Changes That Typify Snake Fungal Disease. *mBio.* 2015 Nov 17;6(6):e01534-15.
8. Last LA, Fenton H, Gonyor-McGuire J, Moore M, Yabsley MJ. Snake fungal disease caused by Ophidiomyces ophiodiicola in a free-ranging mud snake (Farancia abacura). *JVDI* . 2016;28(6):709-713.
9. Dolinski AC, Allender MC, Hsiao V, Maddox CW. Systemic *Ophidiomyces ophiodiicola* Infection in a Free-Ranging Plains Garter Snake (*Thamnophis radix*). *Journal of Herpetological Medicine and Surgery* 2014; 24 (1-2): 7–10
10. Ebani VV. Domestic reptiles as source of zoonotic bacteria: A mini review. *Asian Pac J Trop Med*. 2017 Aug;10(8):723-728.

CASE II:

Signalment:
5-year-old, male, Bearded Dragon *(Pogona vitticeps)*.

History:
Three-day history of anorexia, no defecation, and dull mentation. On physical exam: poor body condition score, severe dehydration, and palpable mass in the mid-left coelomic cavity, described as mobile, firm, and ap-

Figure 2-1. Coelomic viscera, bearded dragon. The serosal surface of the stomach has multifocal, confluent, white-tan, firm, variably demarcated nodules, which extended to the adjacent fat pad, mesentery, and small inteolestine (*Photo courtesy of:* Western College of Veterinary Medicine, University of Saskatchewan, https://wcvm.usask.ca/departments/vet-pathology.php)

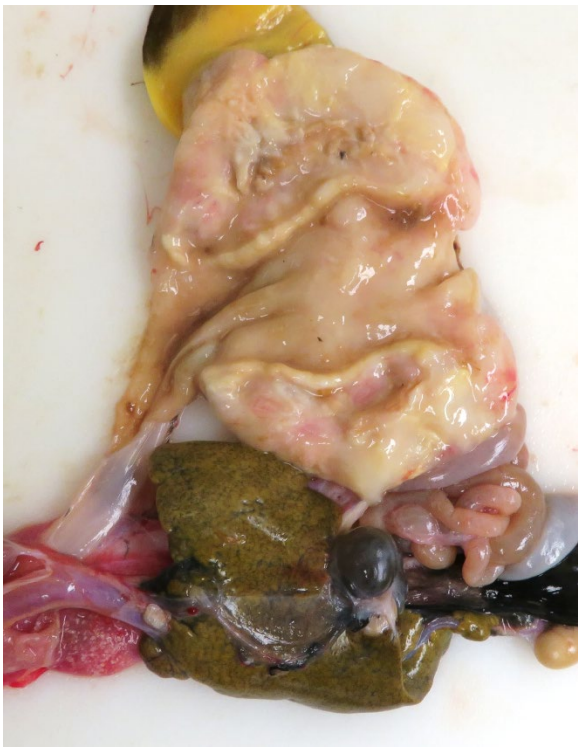

Figure 2-2. Coelomic viscera, bearded dragon. Cut surface of the gastric neoplasm. (*Photo courtesy of:* Western College of Veterinary Medicine, University of Saskatchewan, https://wcvm.usask.ca/departments/vet-pathology.php)

proximately 2 x 4 cm in size. No further diagnostics performed. Euthanasia was elected due to declining condition.

Gross Pathology:
The animal had moderate body fat stores and decreased muscle mass. The mucous membranes of the mouth were pale, and the tongue was pale yellow. The serosal surface of the stomach had multifocal, confluent, white-tan, firm, variably demarcated nodules, which extended to the adjacent fat pad, mesentery, and small intestine. On cut section, the gastric wall was diffusely thickened, white-tan, and firm.

Microscopic Description:
Gastric tumor: Expanding and effacing the gastric submucosa, tunica muscularis, and serosa, there is a well-demarcated, unencapsulated, multi-lobular, infiltrative, and densely cellular neoplasm. The growth is composed of neoplastic polygonal cells arranged in packets, sheets, and occasional pseudorosettes with nuclear palisading around blood vessels, all supported by a delicate fibrovascular stroma. The neoplastic cells have scant, poorly defined, amphophilic, finely granular cytoplasm; their nuclei are round to oval with finely stippled chromatin, and small to inconspicuous nucleoli. There is mild to moderate anisocytosis and anisokaryosis. A total of 37 mitotic figures (sometimes atypical) are counted in 10 consecutive HPF (x400). Many lymphatic vessels are occluded by neoplastic cells. There are multifocal areas of necrosis characterized by eosinophilic cellular and basophilic karyorrhectic debris and eosinophilic smooth to slightly fibrillar deposits (fibrin); sometimes intermixed with colonies of coccobacilli. There are numerous apoptotic cells and variably sized aggregates of granulo-

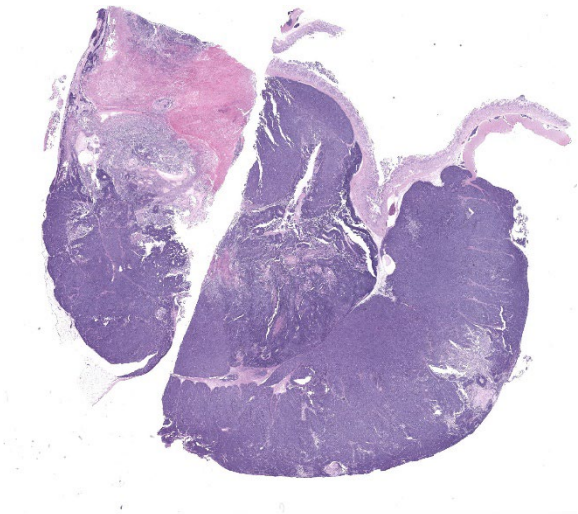

Figure 2-3. Stomach, bearded dragon. Two sections of a large partially necrotic neoplasm arising in the muscularis is submitted for examination. The gastric mucosa is present at top right. (HE, 6X).

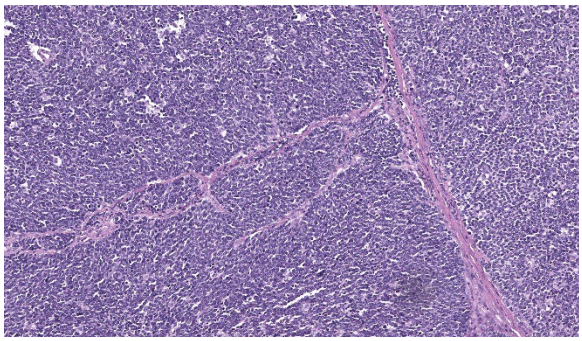

Figure 2-4. Stomach, bearded dragon. Neoplastic cells are arranged in large nests. (HE, 243X).

cytes, lymphocytes, macrophages, and plasma cells within the mass. The gastric mucosal epithelium and glands are usually spared. Approximately 10% of the neoplastic cells have argyrophilic cytoplasmic granules (confirmed with Grimelius stain).

Immunohistochemistry (IHC) for somatostatin on section of gastric tumor: cytoplasmic immunoreactivity in approximately 10% of neoplastic cells.

Contributor's Morphologic Diagnosis:
Gastric neuroendocrine carcinoma (suspected malignant somatostatinoma)

Contributor's Comment:
Neuroendocrine (NE) tumors (also called carcinoids) of the alimentary tract arise from dispersed enteroendocrine cells.[5] There are many types of enteroendocrine cells which have differences in anatomic location and hormonal mediator produced (e.g. G cells are located in the pylorus and produce gastrin), and NE tumors can be further subclassified based on these properties. NE tumors may be benign or malignant, well-differentiated or poorly differentiated, functional or non-functional, and exhibit single or multi-hormonal expression of secretory mediators.[5,9]

Gastric neuroendocrine carcinomas are a highly malignant emerging entity in young bearded dragons, and are frequently metastasized to the liver upon presentation.[9,4,7,11] Commonly observed clinical signs include anorexia, vomiting, weight loss, and lethargy.[4,7,9,11] Reported clinical pathologic abnormalities include hyperglycemia and anemia.[7,9,11] Grossly, gastric tumors are described as variable in size, multinodular but often well demarcated, pale tan to white, firm, with protrusion into the gastric lumen and ulceration of the associated gastric mucosa.[9] Occasional cases report no masses identified grossly.[9] Histopathology of these tumors are characteristic of neuroendocrine neoplasms, and they are primarily located in the gastric submucosa.[4,7,9,11] In one publication, extended IHC analysis of five cases revealed consistent immunoreactivity for somatostatin (n=5), along with varying immunoreactivity for gastrin (n=3), synaptophysin (n=2), pancreatic polypeptide (n=2), chromogranins A and B (n=1), and glucagon (n=1); and therefore further characterized the neoplasms as malignant somatostatinomas.[9]

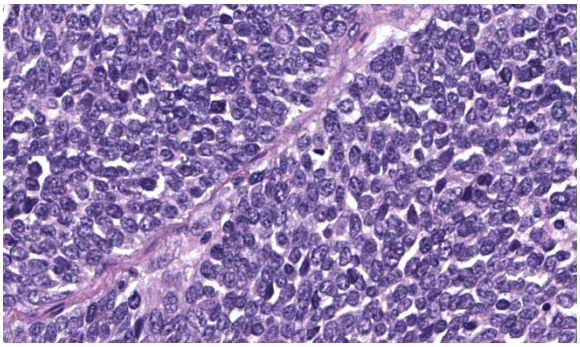

Figure 2-5. Stomach, bearded dragon. High magnification of neoplastic cells. (HE, 1168X).

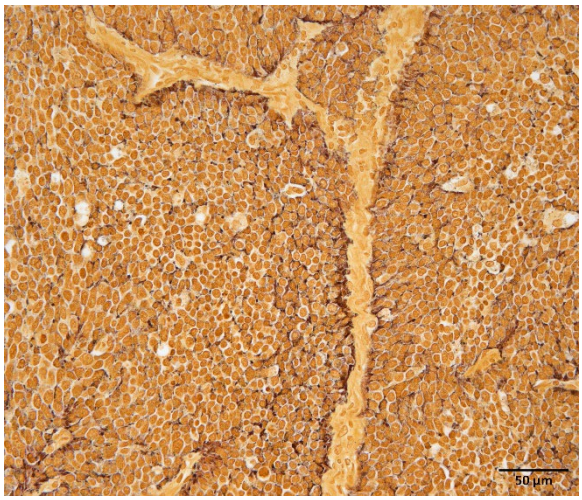

Figure 2-6. Stomach, bearded dragon. A silver stain demonstrates argyrophilic granules within neoplastic cells. (Grimelius, 400X). (*Photo courtesy of:* Western College of Veterinary Medicine, University of Saskatchewan, https://wcvm.usask.ca/departments/vet-pathology.php)

In our individual, there was widespread microscopic metastasis in the heart, lung, liver (with concurrent hepatic lipidosis), small intestine, kidney, adrenal gland, and testes. Cytoplasmic immunoreactivity for somatostatin was observed in a proportion of neoplastic cells and is similarly supportive of a more specific diagnosis of malignant somatostatinoma. However, IHC for other hormonal mediators was not pursued in our case, so the possibility of multi-hormonal expression was not assessed.

Hyperglycemia has been observed in some bearded dragons with these tumors[9,7,11] and is also noted in a proportion of people with somatostatinomas.[6] The pathogenesis of hyperglycemia is due to excessive production of somatostatin, which inhibits secretion of most pancreatic and gut hormones including insulin, leading to decreased glucose intake into cells and therefore elevation of glucose levels in the blood. In people, clinical disease due to excessive somatostatin production from NE tumors is called "somatostatin syndrome", and is characterized by diabetes mellitus, cholelithiasis, and diarrhea/steatorrhea.[6] It is possible that a similar syndrome is occurring in bearded dragons with gastric neuroendocrine carcinomas, however further investigation is needed.

In terms of comparative pathology, gastric NE tumors have been rarely reported in the dog,[3,5,8] cat,[5,10] and ferret.[1] In addition, there is a published case series of benign gastric NE tumors in three captive snow leopards.[2]

Contributing Institution:
Western College of Veterinary Medicine
University of Saskatchewan
52 Campus Dr, Saskatoon, SK, Canada S7N 5B4
https://wcvm.usask.ca/departments/vet-pathology.php

JPC Diagnosis:
Stomach: Neuroendocrine carcinoma

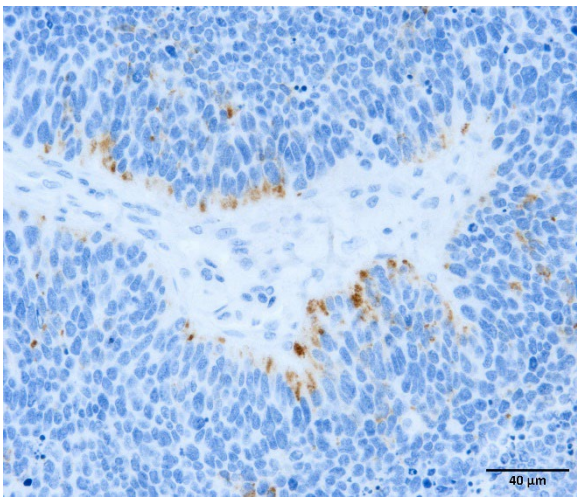

Figure 2-7. Stomach, bearded dragon. Multifocally, neoplastic cells demonstrate strong cytoplasmic immunopositivity for somatostatin. (anti-somatostatin, 400X). (*Photo courtesy of:* Western College of Veterinary Medicine, University of Saskatchewan, https://wcvm.usask.ca/departments/vet-pathology.php).

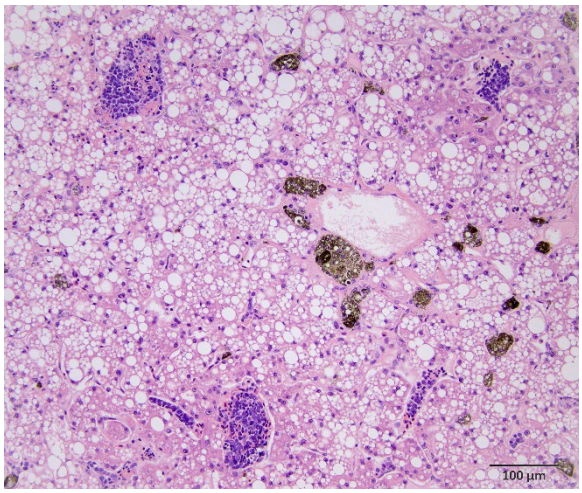

Figure 2-8. Liver, bearded dragon. There is hepatic metastasis. Hepatocytes demonstrate marked lipidosis. (HE, 400X). (*Photo courtesy of:* Western College of Veterinary Medicine, University of Saskatchewan, https://wcvm.usask.ca/departments/vet-pathology.php).

JPC Comment:
Case 2 is a classic neuroendocrine neoplasm in a bearded dragon. We attempted to characterize it further, although the JPC's IHCs (aside from a weakly reactive chromogranin) were negative or non-contributory. Dr. Peiffer emphasized the need for an antibody-specific control in addition to a species tissue control in evaluating the performance of assays that have not been validated in a particular species. This is a frequent consideration for us given that we share laboratory services with a larger human hospital, and few of our antibodies have been validated for exotic species. The Grimelius stain employed by the contributor is a creative way to assess for neuroendocrine cells producing CCK or somatostatin as these characteristically lack an argyrophil reaction.[12] That stated, it is difficult to interpret this stain without a matched control to assess stain performance. Finally, conference participants discussed the somatostatin IHC result – we considered whether the lower proportion of immunoreactive cells could reflect a different neuroendocrine neoplasm producing multiple hormones. For this reason, we settled on a neuroendocrine carcinoma as the most appropriate morphologic diagnosis for this case.

The gross images from this case are excellent and merit a short sidebar discussion. Recognizing normal anatomy is critical when interpreting lesions in zoo animals and wildlife. As the liver of reptiles contains melanomacrophages, the darkened color of the liver in this case is normal and is perhaps accentuated by the histologic finding of lipidosis reported by the contributor. Melanomacrophages are pigment-laden macrophages that contain melanin granules, though they may also contain hemosiderin and/or lipofuscin which cannot be distinguished on H&E alone. Melanomacrophages are also present in fish and amphibians. Melanomacrophage hyperplasia is a non-specific feature that can be appreciated microscopically and in some cases, grossly. Conference participants also discussed the abdominal fat pads and far caudal position of the kidneys in this species (not visible in the provided photo, unfortunately).

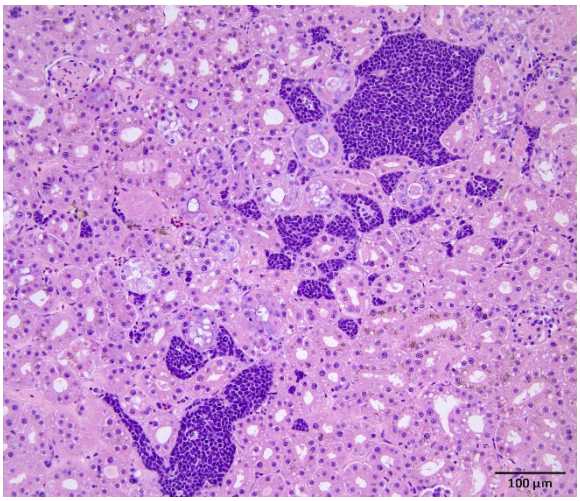

Figure 2-9. Kidney, bearded dragon. There is renal metastasis. (HE, 400X). (*Photo courtesy of:* Western College of Veterinary Medicine, University of Saskatchewan, https://wcvm.usask.ca/departments/vet-pathology.php).

References:

1. Bousquet T, Bravo-Araya M, Davies JL. Gastric neuroendocrine carcinoma (carcinoid) in a ferret *(Mustela putorius furo)*. *Can Vet J*. 2022;63(11):1109-1113.
2. Dobson EC, Naydan DK, Raphael BL et al. Benign gastric neuroendocrine tumors in three snow leopards *(Panthera uncia)*. *J Zoo Wildl Med.* 2013;44(2):441-446.
3. Herbach N, Unterer S, Hermanns W. Gastric neuroendocrine carcinoma in a dog. *Open J Pathol.* 2012;2:162-165.
4. Lyons JA, Newman SJ, Greenacre CB et al. A gastric neuroendocrine carcinoma expressing somatostatin in a bearded dragon *(Pogona vitticeps)*. *J Vet Diagn Invest.* 2010;22:316-320.
5. Munday JS, Löhr CV, Kiupel M. Tumors of the alimentary tract. In: Meuten DJ, 5th edition. *Tumors in domestic animals.* John Wiley & Sons, Inc. 2017:559.
6. Nesi G, Marcucci T, Rubio CA et al. Somatostatinoma: clinico-pathological features of three cases and literature reviewed. *J Gastroenterol Hepatol.* 2008;23(4):521-526.
7. Perpiñán D, Addante K, Driskell E. Gastrointestinal disturbances in a bearded dragon *(Pogona vitticeps)*. *J Herpetol Med Surg.* 2010;20(2-3):54-57.
8. Ovigstad G, Kolbjørnsen Ø, Skancke E et al. Gastric neuroendocrine carcinoma associated with atrophic gastritis in the norwegian lundehund. *J Comp Pathol.* 2008;139(4):194-201.
9. Ritter JM, Garner MM, JA Chilton et al. Gastric neuroendocrine carcinomas in bearded dragons *(Pogona vitticeps)*. *Vet Pathol*. 2009;46:1109-1116.
10. Rossmeisl JH Jr, Forrester SD, Robertson JL et al. Chronic vomiting associated with a gastric carcinoid in a cat. *J Am Anim Hosp Assoc.* 2002;38(1):61-66.
11. Thebeau JM, Martinson SA, Clancey NP et al. Pathology in practice. *J Am Vet Med Assoc.* 2022;259(S2):1-4.
12. Grimelius L. Methods in neuroendocrine histopathology, a methodological overview. Ups J Med Sci. 2008;113(3):243-60.

CASE III:

Signalment:
Adult great blue heron (*Ardea herodias*) of unknown sex

History:
The free-ranging heron was found dead on zoo premises. Blood was noted on the feet.

Gross Pathology:
The heron was in markedly autolyzed postmortem and mildly decreased nutritional condition. Scant dried blood coated the feet. Intracoelomic and pulmonary hemorrhage were present. Embedded in the proventricular and ventricular serosa were seven, 1 mm diameter and 6-11 cm long, tan and red nematodes with tapered tails. A gill raker fragment was firmly embedded in the proventricular mucosa. Firm, cylindrical concretions of feces filled the colon and cloaca.

Laboratory Results:
Cloacal and oropharyngeal swabs were submitted for highly pathogenic avian influenza virus (HPAIV) PCR test. HPAIV was not detected in the sample.

Microscopic Description:
Proventriculus (1 section): The serosa and adjacent adipose are focally disrupted and expanded by a 2.5 mm-diameter granuloma centered on a single, 1 mm-diameter adult nematode that has a smooth eosinophilic cuticle, polymyarian-coelomyarian musculature, hypodermal nuclei, ventral nerve cords, a pseudocoelom, a glandular esophagus with associated pseudomembranes, a reproductive tract, and an intestinal tract lined by uninucleate, columnar epithelium with a

Figure 3-1. Proventriculus and ventriculus, great blue heron. Embedded in the proventricular and ventricular serosa were seven, 1 mm diameter and 6-11 cm long, tan and red nematodes with tapered tails. (*Photo courtesy of:* University of Wisconsin CVM, Dept. of Pathology)

prominent brush border (aphasmid). The nematode is surrounded by large numbers of fragmented heterophils, epithelioid macrophages, and multinucleated giant cells. The granuloma is circumscribed by concentric layers of loose fibrous connective tissue interspersed with many plump fibroblasts and small numbers of lymphocytes. The serosal vessels are multifocally cuffed by medium numbers of lymphocytes and plasma cells. The adipose tissue is severely atrophied. A single proventricular gland is distended by an intraluminal, 0.5 x 1.5 mm adult nematode that has a smooth thin eosinophilic cuticle, indistinct musculature, a pseudocoelom filled with eosinophilic homogeneous material, a reproductive tract containing many embryonated eggs, and an intestinal tract lined by uninucleate columnar epithelium (spirurid). The eggs are 20 x 30 um and ovoid with a smooth, thick shell. Remaining glands multifocally contain eosinophilic flocculent material. The overlying lamina propria is infiltrated by small numbers of eosinophils.

Ventriculus (2 sections): The muscularis and serosa are multifocally disrupted by large, multifocal to coalescing granulomas centered on four sections of an adult aphasmid nematode similar to that previously described in the proventriculus. The granulomas are similarly circumscribed by fibrous connective tissue interspersed with medium numbers of lymphocytes, plasma cells, and eosinophils. The adjacent adipose is severely atrophied.

Contributor's Morphologic Diagnosis:
Proventriculus and ventriculus: Severe, chronic, multifocal to coalescing, granulomatous proventricular serositis and mural ventriculitis with adult aphasmid nematodes

Proventriculus: Moderate, focal glandular ectasia with intraglandular adult spirurid nematode and mild eosinophilic proventriculitis

Contributor's Comment:
Eustrongylidosis is a condition of fish-eating birds caused by infection with aphasmid nematodes in the genus *Eustrongylides*, which has 3 recognized species *E. ignotus, E. tubifex,* and *E. excisus*.[5] *Eustrongylides* spp. are found globally, except for arctic and subarctic regions, and *E. ignotus* and *E. tubifex* are the two species most often reported in the USA.[1,5] Classically, *E. ignotus* affects the ventriculus of Ciconiiformes, whereas *E. tubifex* affects the esophagus and proventriculus of mergansers, loons, and cormorants.[1,2]

For *E. ignotus*, the definitive hosts are multiple genera of herons and egrets in the family Ardeidae.[10] Intermediate hosts include a variety of fish species and oligochaete worms.[2,9] Birds shed eggs into the environment via

their feces, and eggs are consumed by the first intermediate host, an oligochaete worm.[1,5] First and second stage larvae mature within the worm.[5] The first intermediate hosts are then ingested by fish and larvae migrate through the body after penetrating the intestinal wall. Within the fish, larvae mature to the third and fourth stages and can be found in muscle, hepatopancreas, and gonads.[5] Amphibians, reptiles, and predatory fish can also serve as paratenic hosts.[1] Birds then consume parasitized fish or other paratenic hosts and infective fourth stage *Eustrongylides* larvae reach the stomach wall within 3-5 hours of ingestion.[5] Larvae mature over the next 10-15 days, and start producing eggs between 10-25 days post ingestion.[1,5] Eggs are excreted into the environment, where they can survive for several years. [5] Non-patent infections with *E. ignotus* have been reported in Pelecaniformes and non-ardeid Ciconiiforme birds, and birds of prey can also be parasitized.[1,10]

The prevalence of *Eustrongylides* spp. varies between studies and may be related to regional variation in parasite prevalence, increased prevalence in birds submitted to rehabilitation centers or for necropsy, age group studied, and affected avian species. One study in birds at a North California wildlife rehabilitation center found *Eustrongylides* sp. in 30% of necropsied herons and egrets.[6] An earlier study found only 6% of wild nestlings collected from a colony in Northern California were infected, compared to 4% of nestlings in a Rhode Island colony and 35% in a Texas colony.[3]

In affected herons and egrets, low burdens are typically subclinical whereas higher parasite burdens can contribute to individual morbidity and mortality, especially in younger birds.[6] Associated clinical signs include hypothermia, anorexia, regurgitation, weakness, and weight loss.[6,10] Multiple epizootics have been reported in wild Ardeidae, especially in nestlings in coastal rookeries.[1,9] Fatal cases are associated with severe coelomitis and sepsis when penetration of the ventriculus wall by larval eustrongylids leads to bacterial translocation.[2,9]

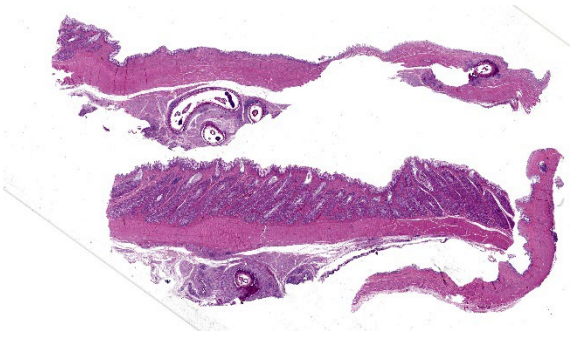

Figure 3-2. Proventriculus and ventriculus, great blue heron. Sections of ventriculus and proventriculus are submitted for examination. There are cross sections of adult aphasmid nematodes within the serosa of the proventriculus, the muscularis of the ventriculus, and an adult spirurid in a proventricular gland. (HE, 10X).

Acute lesions are found in birds as young as 2 days, as well as adults, and are most often associated with fourth-stage larvae, with rarer non-gravid adults.[9] Parasites are typically found below the serosa of the ventricle or on the ventral aspect of the serosal surface.[9] Less often, parasites and/or associated lesions can be found in the air sacs, liver, pericardium, body wall, intestine, or other caudal coelomic organs.[9] Chronic lesions occur in birds over 1 week old, and the majority involve adult parasites.[9] Tortuous, yellow-tan, tubular tunnels containing tan to red nematodes extend across the ventriculus surface, sometimes extending to the intestines and liver.[6,9] Air sacs, gallbladder, proventriculus, cloaca, body wall, and pancreas are less often involved, with esophagus, spleen, kidney and lung rarely affected.[9] More chronic and/or severe cases can have coelomitis, air sacculitis, fibrinous and fibrous adhesions, and inflammatory nodules in multiple organs.[9] For both

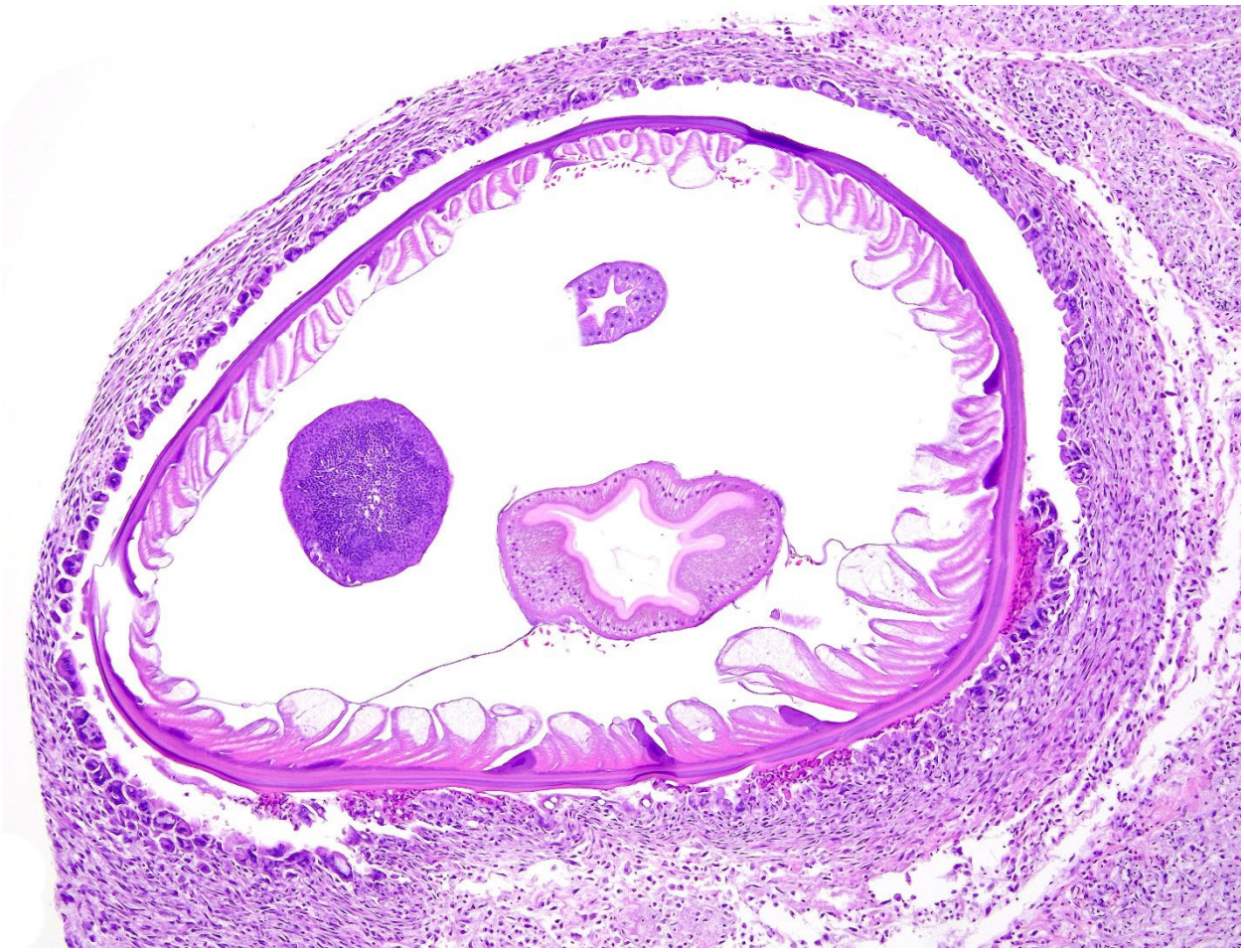

Figure 3-3. Ventriculus, great blue heron. The serosa is expanded by a granuloma centered on a cross-section of adult aphasmid nematode. Features apparent in section include a smooth, eosinophilic cuticle, a pseudocoelom, polymyarian-coelomyarian musculature, and an intestinal tract lined by uninucleate columnar epithelium with a prominent brush border. (HE, 200X) (*Photo courtesy of:* University of Wisconsin CVM, Dept. of Pathology)

acute and chronic cases, a subset are associated with subserosal hematomas.[9]

The most common microscopic findings in acute cases are parasite larvae associated with minimal hemorrhage, eosinophilic inflammation, and pyknotic cellular debris.[9] With chronicity, changes include granulomatous inflammation, necrosis, and fibrosis accompanied by bacterial colonies and eustrongylid eggs.[9] Fibrinous to fibrous tunnels connect to the ventriculus lumen and contain a single, adult parasite, with variable intramural mineralization, eosinophilic infiltrates, and bacteria.[9] Aphasmid nematodes are distinguished by bacillary bands and a single genital tract in adult females.[4] *Eustrongylides* spp. have thick-shelled, operculated eggs, a glandular esophagus, a smooth cuticle, coelomyarian musculature, and pseudomembranes.[4]

In waterbirds, a specific coelomic palpation protocol is a useful antemortem diagnostic technique, especially for more chronic cases with tunnel lesions.[8] Mineralization of parasite tunnels in the ventriculus may be visible radiographically.[10] Post-mortem diagnosis is

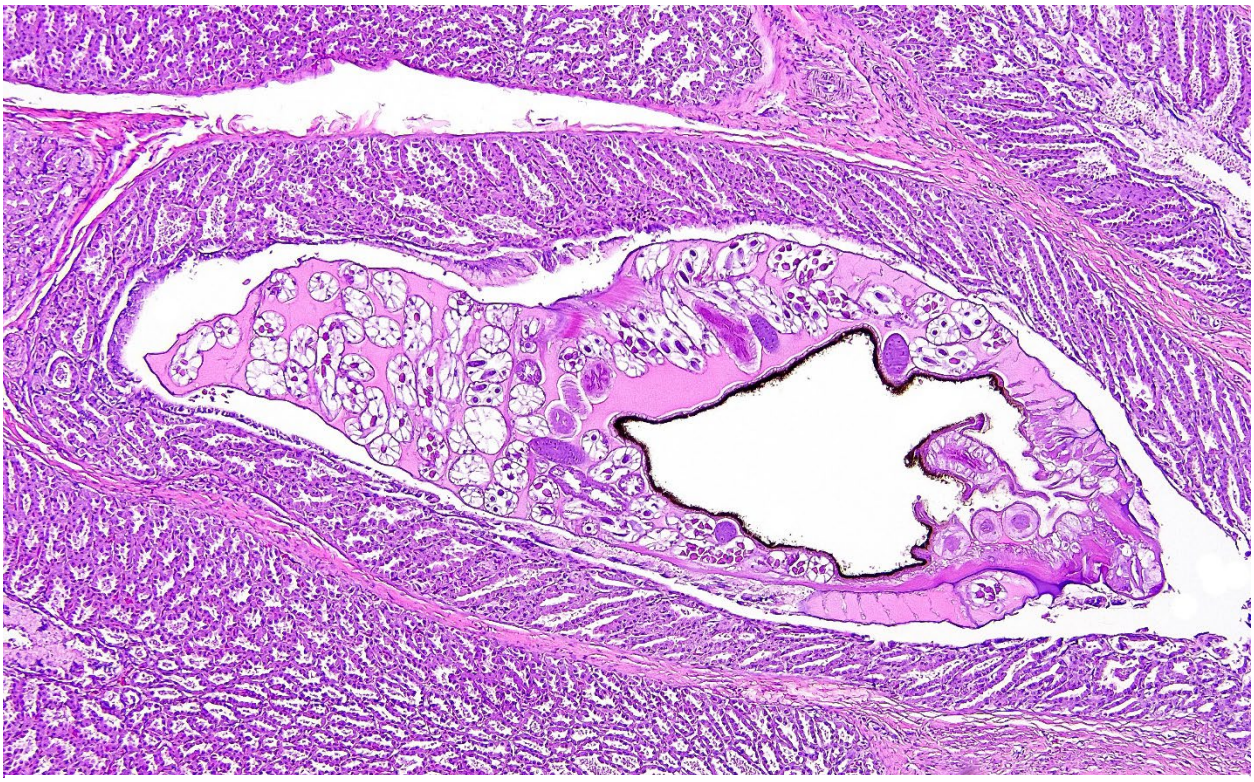

Figure 3-4 Proventriculus, great blue heron. A dilated mucosal gland contains an intraluminal, adult spiurid nematode consistent with *Tetrameres* sp. Features apparent in section include a smooth, thin, eosinophilic cuticle, indistinct musculature, a pseudocoelom filled with eosinophilic, homogeneous material, and reproductive tract with embryonated eggs. (HE, 200X) (*Photo courtesy of:* University of Wisconsin CVM, Dept. of Pathology)

typically by observation of characteristic lesions and identification of larvae or adult parasites, although molecular-genetic techniques are also reported.[5] Human eustrongylidosis is rare, reported most often in the USA in individuals with a history of ingesting live or raw fish.[5]

Tetrameres spp. are spirurid nematodes belonging to the Tetrameridae family, a group which includes three genera (Tetrameres, Microtetrameres, and Geopetitia) and dozens of species.[2,7] For *Tetrameres*, female parasites are found within proventriculus glands; males are either associated with females or within the lumen, although some species encyst within the muscular wall.[7] Sexual dimorphism is a prominent feature for Tetrameridae and females may be globular and less filiform than males due to marked uterine distention.[7] *Tetrameres* lifecycles vary based on species, but the definitive host is usually an aquatic bird and the intermediate host is usually a crustacean.[7] For parasites primarily affecting terrestrial birds, the intermediate host are typically orthopteran or coleopteran insects.[7] Prevalence varies based on species and geographic location; prevalence and intensity can also vary substantially by year and study.[7] Infection is often considered incidental, but overcrowding and high intensity infections can contribute to morbidity and/or mortality.[2] In domestic species, typical clinical signs of *Tetrameres* sp. infection include hyporexia, diarrhea, and emaciation, and

clinical signs in wild birds are less defined.[7] Aquatic birds are most often affected (e.g. Anseriformes, Ardeiformes, Gruiformes, and Charadriiformes), although Passeriformes and Galliformes can be parasitized by some species.[7] *Microtetrameres* spp. more often parasitize terrestrial birds or those feeding on land, whereas *Geopetitia* can parasitize a wide variety of wild birds globally.[7] For this case, *Microtetrameres* sp. remains a differential based on histologic features. Classic gross findings of *Tetrameres* sp. infection include red nodules in the proventricular mucosa containing red, female adult worms, which can be visible from the serosal surface, mucosal hyperplasia, necrotic material coating the proventricular mucosa, mucoid material coating the small intestinal mucosa, and green to golden-brown discoloration of small intestinal contents.[2,7] Histologically, parasites show typical features of spirurid parasites including coelomyarian musculature, large intestines lined by uninucleate cells, eosinophilic fluid within the pseudocoelom, prominent lateral chords, and small characteristic spirurid eggs within adult females.[4] Proventricular glands are distended by adult female nematodes, which can cause compressive changes in adjacent tissue, and there is variable mucosal inflammation.[7] Fecal examination may reveal ovoid, thick-shelled, larvated ova; however, these are challenging to differentiate from other spirurid eggs.[7] Typically, diagnosis is via post-mortem detection of classic lesions and worms, and speciation is primarily via examination of male worms.[7] *Tetrameres* spp. can infect both domestic and wild birds, but is not known to infect humans.[7]

Contributing Institution:
University of Wisconsin
School of Veterinary Medicine
Department of Pathobiological Sciences
2015 Linden Drive
Madison, WI 53706

JPC Diagnosis:
1. Proventriculus and ventriculus: Serositis, granulomatous, diffuse, marked with adult aphasmid nematodes

2. Proventriculus: Glandular ectasia, focal, moderate to marked, with intraglandular adult spirurid nematode

3. Adipose tissue: Atrophy, diffuse, marked

JPC Comment:
We thank the contributor for the detailed writeup and presentation of these two nematodes in section. Identifying *Eustrongylides* was not much of a diagnostic mystery as characteristic structures were easy to appreciate (and its large size helps a bit as well). The single *Tetrameres* was slightly more problematic though careful examination and comparison to *Eustrongylides* allowed conference participants to appreciate the different features. The eosinophilic fluid within the pseudocoelom was helpful as the overall shape of the nematode is not as globoid (or filled with ova) as we have seen previously which may reflect some degeneration. Incidentally, we also noticed the eosinophils the contributor describes in the adjacent portion of the proventriculus. Distinguishing granulocytes is difficult in birds, though the round granules (and adjacent metazoan parasite) are supportive. In contrast, heterophils have more elongate granules. We also added an additional morphologic diagnosis for the atrophy of fat which was quite pronounced in this case.

References:

1. Eustrongylidosis. In: Friend M, Franson JC, eds. Field Manual of Wildlife Diseases: General Field Procedures and Diseases of Birds. US Geological Survey, Biological Resources Division. 1999; 223-228.
2. Fenton H, McManamon R, Howerth EW.

Anseriformes, Ciconiiformes, Charadriiformes, and Gruiformes. In: Terio KA, McAloose D, St Leger J eds. *Pathology of Wildlife and Zoo Animals.* Associated Press; 2019.
3. Franson JC, Custer TW. Prevalence of eustrongylidosis in wading birds from colonies in California, Texas, and Rhode Island, USA. *Col Waterbirds.* 1994;17(2):168-172.
4. Gardiner CH, Poynton SL. In: An Atlas of Metazoan Parasites in Animal Tissues. Armed Forces Institute of Pathology; 1999.
5. Honcharoy SL, Soroka NM, Galat MV, Zhurenko OV, Dubovyi AI, Dzhmil VI. *Eustrongylides* (Nematoda: Dioctophymatidae): Epizootiology and special characteristics of the development biology. *Helminthologia*. 2022;59(2):127-142.
6. Horgan M, Duerr R. Gross pathology of herons and egrets (family Ardeidae) at a wildlife rehabilitation centre in Northern California. *J Wildl Rehabil.* 2021;37(1):29-41.
7. Kinsella JM, Forrester DJ. Tetrameridosis. In: Atkinson CT, Thomas NJ, Hunter DB, eds. *Parasitic Diseases of Wild Birds*. John Wiley & Sons; 2008.
8. Spalding MG. Antemortem diagnosis of eustrongylidosis in wading birds (Ciconiiformes). *Col Waterbirds*. 1990;13(1):75-77.
9. Spalding MG, Bancroft GT, Forrester DJ. The epizootiology of eustrongylidosis in wading birds (Ciconiiformes) in Florida. *J Wildl Dis*. 1993;29(2):237-249.
10. Spalding MG, Forrester DJ. Pathogenesis of *Eustrongylides ignotus* (Nematoda: Dioctophymatoidea) in Ciconiiformes. *J Wildl Dis.* 1993;29(2):250-260.

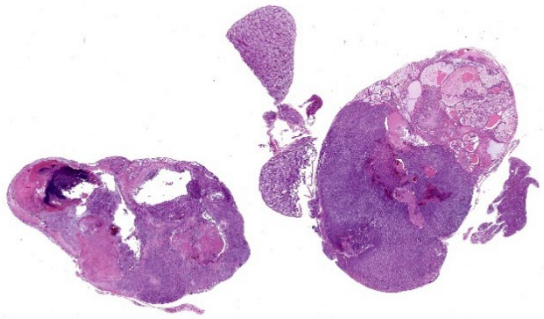

Figure 4-1. Kidney, budgerigar. Multiple sections of a kidney which is effaced by a neoplasm are submitted for examination. Normal testis is also present (center) (HE, 6X)

CASE IV:

Signalment:
Adult, male, blue and white budgerigar (*Melopsittacus undulatus*)

History:
This adult male budgerigar was housed in an indoor aviary. He had been vaccinated against West Nile virus in May, 2020. Spring of 2021, he was found dead with no reported antemortem clinical signs.

Gross Pathology:
Bilaterally effacing the kidneys is a multilobulated, poorly circumscribed, tan, soft mass. The mass moderately displaces the testes, cranially. There are scant subcutaneous and visceral adipose stores.

Laboratory Results:
Chlamydia psittaci, avian polyomavirus, and psittacine herpesvirus were not detected by real time PCR on pooled lung, liver, and kidney samples.

Microscopic Description:
Kidney, left and right: Expanding and effacing both examined sections of kidney is a large, multinodular, unencapsulated, densely cellular infiltrative neoplasm. The polygonal neoplastic cells variably form haphazardly organized tubules, papillary proliferations,

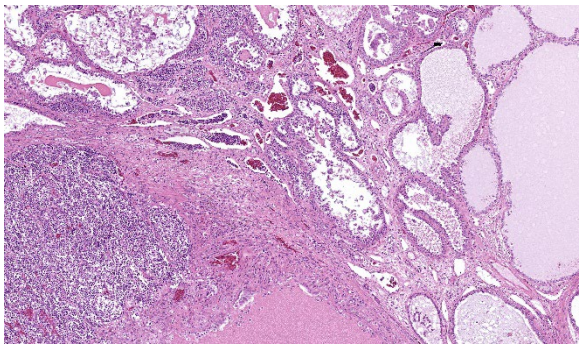

Figure 4-2 Kidney, budgerigar. The neoplasm is composed of cuboidal epithelium forming viarbly dilated tubules. A large amount of the tumor is composed of tumor cells in sheets (lower left). (HE, 154X)

and occasional cords arranged over a fine fibrovascular stroma. The neoplastic epithelial cells have distinct cell borders, scant to moderate amounts of clear to granular eosinophilic cytoplasm, and a single, basally to centrally located round nucleus with finely stippled chromatin and one variably distinct amphophilic to eosinophilic nucleolus. There is mild to moderate anisocytosis and anisokaryosis. There is approximately one mitotic figure per high power (400x) field. There are large multifocal regions of necrosis and hemorrhage with hemosiderin laden macrophages and heterophils scattered throughout the neoplasm. Mild to moderate amounts of bright homogenous eosinophilic material (proteinaceous fluid) occasionally fills neoplastic and remaining normal renal tubular lumina. The remaining normal renal parenchyma is compressed at the periphery of the mass. The remaining pre-existing renal tubules occasionally exhibit one or more of the following changes: mild to moderate ectasia, epithelial attenuation, pale vacuolated eosinophilic cytoplasm with loss of cellular detail (degeneration), and/or colorless to basophilic radiating, sharp, acicular, crystalline deposits (urate tophi), often accompanied and surrounded by heterophils and macrophages.

Contributor's Morphologic Diagnosis:
Kidney: Renal adenocarcinoma, budgerigar

Contributor's Comment:
The cellular morphology and arrangement of the mass in this case are characteristic of renal tubular epithelial origin.

Renal carcinomas and adenomas are significantly more common in budgerigars than other psittacine species, although the mechanisms for this are not completely understood.[6] Captive birds are generally understood to have a higher incidence of neoplasia than wild birds, potentially due to differences in life span, diet, and carcinogen exposure.[8] Several carcinogens, including but not limited to aflatoxins, lead, and nitrosamines, are thought to contribute to renal carcinoma development in veterinary species.[4] In addition to carcinogen exposure, several viral etiologies have been identified in renal carcinomas in some species, including induction of renal adenocarcinoma via avian erythroblastosis virus in chickens[1] and renal adenocarcinomas, also known as Lucké's tumor of leopard frogs, by ranid herpesvirus type 1 (RaHV-1).[3] Investigations into potential retroviral causes of renal neoplasms in budgerigars have not identified associated retroviruses.[7]

The most frequent presenting clinical sign of renal adenocarcinoma in birds is unilateral lameness due compression of the sciatic nerve.[8] The gross appearance of the renal adenocarcinoma in this case was very characteristic. Most renal adenocarcinomas are large, tan to reddish brown, soft to friable, and are located at the cranial pole of the kidneys (in this case, displacing the testes cranially).[8] Histologically, the variation in arrangement of tubules, papillary projections and more solid areas of tightly packed cords confirm the suspected diagnosis of renal cell adenocarcinoma. Renal adenomas have less cellular pleomorphism and are comprised of tubules lined by a single layer of epithelium with a moderate fibrovascular stroma. Avian renal carcinomas and adenocarcinomas are

reported to infrequently metastasize to the lungs and liver.[6]

A majority of the immunohistochemical characterization of renal adenocarcinomas and renal cell carcinomas has been done in canine patients. Immunohistochemistry for uromodulin and uroplakin may be useful for confirming tissue of renal origin, as these markers are commonly expressed by canine renal tumors.[2] Additionally, canine renal cell carcinomas frequently co-express cytokeratin and vimentin, and express CD10, PAX 8, and napsin A.[5] Though no immunohistochemistry was pursued in this case, it may be useful to try the above-mentioned markers in renal tumors from budgies if the diagnosis based only on morphology is in question.

In contrast to budgerigars, primary renal neoplasms are uncommon in most domestic veterinary species. The most common primary renal neoplasm in dogs, cats, cattle, and horses are renal cell carcinomas rather than adenocarcinomas. Additional differential diagnoses for a primary renal mass include renal adenoma, oncocytoma, and transitional cell papilloma and carcinoma. Renal adenomas are rare, benign epithelial neoplasms which are not commonly reported in budgerigars.[1]

Contributing Institution:
University of Wisconsin
School of Veterinary Medicine
Department of Pathobiological Sciences
2015 Linden Drive
Madison, WI 53706

JPC Diagnosis:
Kidney: Renal adenocarcinoma

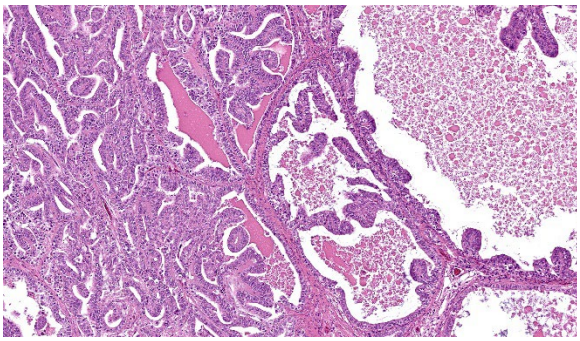

Figure 4-3. Kidney, budgerigar. In some ectatic tubules, neoplastic cells form intricate papillary projections. (HE, 154X)

JPC Comment:
The final case of this conference is another classic neoplasm, this time in a budgie. The contributor gave us several options among slides for this case. The digital section that we ultimately chose has a great assortment of ancillary features, though it might initially be misleading on tissue identification with the normal testis distracting from the relatively small portion of remaining renal cortex to evaluate. We agree that this neoplasm is a renal adenocarcinoma that has both solid and papillary-predominant regions mixed with necrotic foci. In solid regions, neoplastic cells have increased cytoplasmic clearing which has been described as a clear cell histologic subtype.

We took the contributor up on their challenge to try canine renal cell carcinoma markers for this case. Napsin A, CD10, CK7, vimentin, and uroplakin were all immunonegative. We noted moderate-to-strong nuclear immunoreactivity to PAX8 within 30% of neoplastic cells (predominately in well-differentiated cells in the papillary-predominant region), consistent with renal epithelial cell origin. This distribution also aligns with PAX8 performance in canine RCCs.[5] The remaining renal tubules served as a useful internal tissue control. That stated, there is conflicting information that the avian genome (or at least chickens) lack an orthologous *Pax8* gene[9] despite this convincing antibody performance.

Polyclonal PAX8 antibodies do cross label with PAX5 – review of lab materials indicate that we used a monoclonal mouse primary antibody (MRQ-50; Ventana) which removes this possibility. We look forward to trying this antibody with appropriate controls in future cases (see discussion in case 2 of this conference) should the opportunity arise.

References:

1. Breshears MA, Confer AW. The Urinary System. In: Zachary JF ed. *Pathologic Basis of Veterinary Disease*. 6th ed. Elsevier; 2017.
2. Cianciolo RE, Mohr FC. Urinary System. In: Maxie MG ed. *Jubb, Kennedy, and Palmer's Pathology of Domestic Animals*. 6th ed. Elsevier; 2016.
3. McKinnel RG, Carlson DL. Lucke renal adenocarcinoma, an anuran neoplasm: Studies at the interface of pathology, virology, and differentiation competence. *J Cell Physiol.* 1997;173:115-118.
4. Meuten DJ, Meuten TLK. Tumors of the Urinary System. In: Meuten DJ ed.T*umors in Domestic Animals.* 5th ed. John Wiley & Sons, Inc; 2017.
5. Peat TJ, Edmondson EF, Miller MA, DuSold DM, Ramos-Vara JA. Pax8, Napsin A, and CD10 as immunohistochemical markers of canine renal cell carcinoma. *Vet Pathol*. 2017;54:588-594.
6. Schmidt RE, Reavill DR, Phalen DN. *Pathology of Pet and Aviary Birds*. Iowa State Press; 2003.
7. Simova-Curd SA, Huder JB, Boeni J, Robert N, Hatt JM. Investigations on the diagnosis and retroviral aetiology of renal neoplasia in budgerigars (*Melopsittacus undulatus*). *Avian Pathol.* 2010;39:161-167.
8. Simova-Curd S, Nitzl D, Mayer J, Hatt JM. Clinical approach to renal neoplasia in budgerigars (*Melopsittacus undulatus*). *J Small Anim Pract*. 2006;47:504-511.
9. Freter S, Muta Y, O'Neill P, Vassilev VS, Kuraku S, Ladher RK. Pax2 modulates proliferation during specification of the otic and epibranchial placodes. Dev Dyn. 2012 Nov;241(11):1716-28.